Efficient three-photon luminescence with strong polarization dependence from a scintillating silicate glass co-doped with Gd^{3+} and Tb^{3+}

Guang-Can Li,[1] Cheng-Yun Zhang,[1] Hai-Dong Deng,[1] Guang-Yin Liu,[1] Sheng Lan,[1,*] Qi-Qian,[2] Zhong-Min Yang,[2] and Achanta Venu Gopal[3]

[1]*Laboratory of Nanophotonic Functional Materials and Devices, School of Information and Optoelectronic Science and Engineering, South China Normal University, Guangzhou 510006, China*
[2]*MOE Key Laboratory of Specially Functional Materials, Institute of Optical Communication Materials, South China University of Technology, Guangzhou 510640, China*
[3]*Department of Condensed Matter Physics and Material Science, Tata Institute of Fundamental Research, Homi Bhabha Road, Mumbai 400005, India*
[*]*slan@scnu.edu.cn*

Abstract: Efficient three-photon luminescence (3PL) from a scintillating silicate glass co-doped with Gd^{3+} and Tb^{3+} was generated by using a focused femtosecond laser beam at 800 nm. Four emission bands centered at 496, 541, 583, and 620 nm were identified as the electronic transitions between the energy levels of Tb^{3+} followed by three-photon absorption (3PA) in Gd^{3+} and Tb^{3+} and the resonant energy transfer from Gd^{3+} to Tb^{3+}. More interestingly, a strong polarization dependence of the 3PL was observed and it is ascribed to the polarization dependent 3PA in Gd^{3+} and Tb^{3+} and/or the angular distribution of photogenerated electrons in the glass.

OCIS codes: (190.4180) Multiphoton processes; (160.5690) Rare-earth-doped materials; (190.7220) Upconversion.

References and links

1. G. Zanella, R. Zannoni, R. Dall'Igna, B. Locardi, P. Polato, M. Bettinelli, and A. Marigo, "A new cerium scintillating glass for X-ray detection," Nucl. Instr. Meth. A **345**(1), 198–201 (1994).
2. D. F. Anderson, "Properties of the high-density scintillator cerium fluoride," EEE Trans. Nucl. Sci. **36**(1), 137–140 (1989).
3. G. Zanella and R. Zannoni, "The detective quantum efficiency of an imaging detector," Nucl. Instr. Meth. A **359**(3), 474–477 (1995).
4. C. Pedrini, B. Moine, J. C. Gacon, and B. Jacquier, "One- and two-photon spectroscopy of Ce^{3+} ions in LaF_3-CeF_3 mixed crystals," J. Phys. Condens. Matter **4**(24), 5461–5470 (1992).
5. M. Nikl and C. Pedrini, "Photoluminescence of heavily doped CeF_3:Cd^{2+} single crystals," Solid State Commun. **90**(3), 155–159 (1994).
6. M. Nikl, "Scintillation detectors for X-rays," Meas. Sci. Technol. **17**(4), R37–R54 (2006).
7. M. C. Aznar, C. E. Andersen, L. Bøtter-Jensen, S. Å. J. Bäck, S. Mattsson, F. Kjaer-Kristoffersen, and J. Medin, "Real-time optical-fibre luminescence dosimetry for radiotherapy: physical characteristics and applications in photon beams," Phys. Med. Biol. **49**(9), 1655–1669 (2004).
8. W. P. Siegmund, P. Nass, J. P. Fabre, W. Flegel, V. Zacek, G. Martellotti, and G. Wilquet, "Glasses as active and passive components for scintillating fiber detectors," SPIE **1737**, 2–13 (1993).
9. J. A. Mares, M. Nikl, K. Nitsch, N. Solovieva, A. Krasnikov, and S. Zazubovich, "A role of Gd^{3+} in scintillating process in Tb-doped Na-Gd phosphate glasses," J. Lumin. **94–95**, 321–324 (2001).
10. D. He, C. Yu, J. Cheng, S. Li, and L. Hu, "Energy transfer between Gd^{3+} and Tb^{3+} in phosphate glass," J. Rare Earths **29**(1), 48–51 (2011).
11. G. H. Dicke, *Spectra and Energy Levels of Rare-Earth Ions* (Wiley, 1968).
12. S. Zhang, B. Zhu, S. Zhou, S. Xu, and J. Qiu, "Multi-photon absorption upconversion luminescence of a Tb^{3+}-doped glass excited by an infrared femtosecond laser," Opt. Express **15**(11), 6883–6888 (2007).
13. A.-H. Li, Z. R. Zheng, Q. Lü, L. Sun, W.-Z. Wu, W.-L. Liu, Y.-Q. Yang, and T.-Q. Lü, "Two-photon-excited luminescence in a Tb^{3+} -doped lithium niobate crystal pumped by a near-infrared femtosecond laser," Opt. Lett. **33**(9), 1014–1016 (2008).
14. K. Hanaoka, K. Kikuchi, S. Kobayashi, and T. Nagano, "Time-Resolved long-lived luminescence imaging method employing luminescent lanthanide probes with a new microscopy system," J. Am. Chem. Soc. **129**(44), 13502–13509 (2007).

#181857 - $15.00 USD Received 21 Dec 2012; revised 18 Feb 2013; accepted 23 Feb 2013; published 4 Mar 2013

15. K. L. Wong, W. M. Kwok, W. T. Wong, D. L. Phillips, and K. W. Cheah, "Green and red three-photon upconversion from polymeric lanthanide(III) complexes," Angew. Chem. Int. Ed. Engl. **43**(35), 4659–4662 (2004).
16. H. C. Aspinall, "Chiral lanthanide complexes: coordination chemistry and applications," Chem. Rev. **102**(6), 1807–1850 (2002).
17. S. Wang, Q. Qian, Q. Y. Zhang, Z. M. Yang, and Z. H. Jiang, "Gd^{3+}-sensitized Tb^{3+}-doped scintillating silicate glasses," J. Inor. Materi. **24**(4), 773–777 (2009).
18. J. Fu, M. Kobayashi, and J. M. Parker, "Terbium-activated heavy scintillating glasses," J. Lumin. **128**(1), 99–104 (2008).
19. M. C. Downer and A. Bivas, "Third- and fourth-order analysis of the intensities and polarization dependence of two-photon absorption lines of Gd^{3+} in LaF_3 and aqueous solution," Phys. Rev. B **28**(7), 3677–3696 (1983).
20. R. Francini, U. M. Grassano, S. Boiko, G. G. Tarasov, and A. Scacco, "Anisotropy of two-photon excited f-f transitions of Eu^{2+} in $KMgF_3$," J. Chem. Phys. **110**(1), 457–464 (1999).
21. M. C. Downer, C. D. Cordero-Montalvo, and H. Crosswhite, "Study of new $4f^7$ levels of Eu^{2+} in GaF_2 and SrF_2 using two-photon absorption spectroscopy," Phys. Rev. B **28**(9), 4931–4943 (1983).
22. H. J. Seo, B. K. Moon, and T. Tsuboi, "Two-photon excitation spectroscopy of $4f^7$-$4f^7$ transitions of Eu^{2+} ions doped in a $KMgF_3$ crystal," Phys. Rev. B **62**(19), 12688–12695 (2000).
23. P. G. Kazansky, H. Inouye, T. Mitsuyu, K. Miura, J. Qiu, K. Hirao, and F. Starrost, "Anomalous anisotropic light scattering in Ge-doped silica glass," Phys. Rev. Lett. **82**(10), 2199–2202 (1999).

1. Introduction

Owing to their potential applications in high-energy and nuclear physics, medical imaging, and industry, scintillators and especially rare-earth-ion-doped glasses have attracted great interest in the last two decades because such glasses can be fabricated at a low cost and in large quantities [1–5]. More importantly, optical fibers made of these glasses will further broaden their applications in the fields of thermal neutron detection and radiography, nondestructive testing, and radiation dosimetry [6–8].

In the research and development of scintillating glasses, Terbium-doped glasses have been the focus of many studies because of their high luminescence efficiency at around 550 nm which is convenient for direct coupling with silicon detectors [6]. Being as important as scintillating materials, Tb^{3+}-doped glasses and fibers have been used in nondestructive testing and high-resolution medical imaging [8]. More interestingly, it has been shown that the luminescence can be further enhanced by adding Gd^{3+} into Tb^{3+}-doped glasses because of the resonant energy transfer (RET) from Gd^{3+} to Tb^{3+} [9,10]. In contrast to the intensive and extensive studies of scintillating glasses by using high-energy radiation such as ultravoilet or X ray, less attention has been paid to their nonlinear optical properties such as the up-converted processes produced by femtosecond (fs) laser pulses in the near infrared region. In fact, these glasses are favorable candidates for the generation of short wavelength radiation through multiphoton absorption (MPA) because rare-earth ions possess numerous energy levels in the infrared, visible and ultraviolet regions [11–13]. In addition, the excited states of rare-earth ions generally have long lifetimes [14,15], which also support stepwise excitation in MPA. The efficient upconversion in combination with the long lifetimes of these rare-earth ions make them attractive for imaging of life cells with no autofluent background and photobleaching [13].

In this article, we investigate the multiphoton-induced luminescence (MPL) of a scintillating silicate glass co-doped with Gd^{3+} and Tb^{3+} by using a focused fs laser beam. The composition of the glass is $56SiO_2$-$10Al_2O_3$-$12Li_2O$-$20Gd_2O_3$-$2Tb_2O_3$ (mol%) and the detailed fabrication process can be found in a previous publication [16]. The dependence of the luminescence intensity on the excitation density and especially polarization was examined. The physical mechanism responsible for the MPL and its polarization dependence was proposed.

2. Experimental details

The experimental setup used to study the MPL of the glass and its polarization dependence is schematically shown in Fig. 1. The 800-nm fs laser light with a repetition rate of 76 MHz and a pulse duration of ~120 fs delivered by a Ti: sapphire oscillator (Mira 900, Coherent) was introduced into an inverted microscope (Observer A1, Zeiss), reflected by a dichroic mirror

#181857 - $15.00 USD Received 21 Dec 2012; revised 18 Feb 2013; accepted 23 Feb 2013; published 4 Mar 2013

and focused on the glass, which has been polished, by using a 40 × objective lens (NA = 0.65). The diameter of the excitation spot was estimated to be ~4.4 μm. The luminescence from the glass was collected by the same objective lens and delivered to a spectrometer (SR-500I-B1, Andor) equipped with a charge-coupled device (CCD) (DU970N, Andor) for analysis. The polarization of the fs laser light was modified by using a half-wave (λ/2) plate while its intensity was adjusted by using an attenuator.

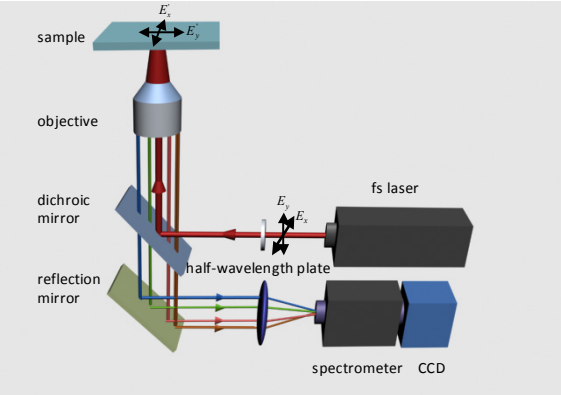

Fig. 1. Experimental setup used to generate the MPL from the scintillating glass and to investigate its dependence on the polarization of the fs laser light.

3. Results and discussion

3.1 Single-photon-induced luminescence from the glass

Before studying the MPL of the glass, we first examined the emission and excitation spectra of the glass under single photon excitation by using a fluorescence spectrometer (F-4500, Hitachi). They are shown in Fig. 2(a) by the black solid curve and dark blue dashed curve, respectively. In the emission spectrum obtained by single photon excitation at 253 nm, one can see four narrow emission bands centered at 496, 541, 583, and 620 nm which have been observed in glasses of different compositions co-doped with Tb^{3+} and Gd^{3+} under the excitation of ultraviolet or X ray [16–19]. They have been attributed to the electronic transitions between the energy levels of Tb^{3+} (i.e., $^5D_4 \rightarrow {}^7F_6$, $^5D_4 \rightarrow {}^7F_5$, $^5D_4 \rightarrow {}^7F_4$, and $^5D_4 \rightarrow {}^7F_3$), as depicted in Fig. 3. Although Gd^{3+} was doped in the glass in a large amount, we did not see any emission from Gd^{3+}. In the excitation spectrum obtained by monitoring the luminescence intensity at 549 nm, one can see a broad band with a strong intensity ranging from ~240 to ~280 nm, implying a high efficiency for three-photon absorption (3PA) by using fs laser at ~800 nm.

3.2 Three-photon-induced luminescence from the glass

In Fig. 2(a), we also show the MPL spectra of the glass obtained at 800 nm for different excitation densities by colored curves. The excitation densities given in Fig. 2 are average power densities obtained by dividing the average powers of the fs laser with the area of the excitation spot. The corresponding peak power densities can be readily deduced and they are several orders of magnitude larger than the average power densities. Similarly, four narrow emission bands centered at 496, 541, 583, and 620 nm are observed. However, the relative intensities of the four emission bands (2.96: 7.81: 1.13: 1) are found to be different from those observed in single photon excitation (5.90: 14.31: 1.56: 1).

#181857 - $15.00 USD Received 21 Dec 2012; revised 18 Feb 2013; accepted 23 Feb 2013; published 4 Mar 2013

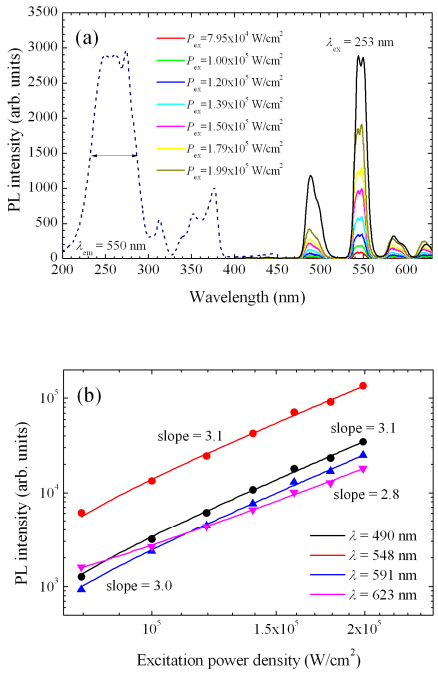

Fig. 2. (a) Emission and excitation spectra of the glass under single photon excitation and its MPL spectra under different excitation densities at 800 nm. (b) Logarithmic plots of the PL peak intensity versus excitation density for the four different emission bands along with fits.

In order to gain a deep insight into the nonlinear process involved in the MPL of the glass, the excitation density dependence of the luminescence intensity at the central wavelength of each emission band was analyzed and the results are presented in Fig. 2(b). The fitting of the excitation density dependent luminescence gives a power index of ~3 for all emission bands, indicating that 3PA is responsible for the generation of the luminescence. As far as 3PA processes are concerned, there are three possible ways. One is the stepwise excitation to a high-energy level by continuously absorbing three photons. This process requires the existence of equally separated energy levels with energy interval equal to the one-photon energy of the pump light. Another is one-photon excitation to a real level followed by a two-photon absorption (2PA) or two-photon excitation to a real level followed by one-photon absorption. The third is the simultaneous absorption of three photons. From the energy level diagrams of Gd^{3+} and Tb^{3+} presented in Fig. 3, it can be clearly seen that there are not two energy levels whose energy interval equals to the one- or two-photon energy of the pump light. It is further confirmed by the absorption spectrum of the 0.5-mm-thick glass shown in Fig. 4. In the insets of Fig. 4 where the magnified violet and visible spectral regions are shown, one can identify three tiny peaks which can be attributed to the absorptions in Gd^{3+} and Tb^{3+}. The red and green arrows indicate the absorptions in Gd^{3+} due to the electronic transitions $^8S_{7/2} \rightarrow {}^6I_J$ (J = 11/2, 13/2, 15/2) and $^8S_{7/2} \rightarrow {}^6P_{7/2}$, respectively. The corresponding wavelengths appear at ~273 nm and ~312 nm. The blue arrow indicates the absorption in Tb^{3+} due to the electronic transition $^7F_6 \rightarrow {}^5D_4$, corresponding to a wavelength of ~490 nm. On the other hand, the energy of three photons, which corresponds to a central wavelength of ~267 nm, matches approximately the energy interval for the electronic transition $^8S_{7/2} \rightarrow {}^J I_6$ in Gd^{3+} (~273 nm) and the electronic transition $4f^8 \rightarrow 4f^7 5d^1$ in Tb^{3+} (~281 nm) [16]. Therefore, it is thought that the three-photon luminescence (3PL) of the glass originates from the

#181857 - $15.00 USD Received 21 Dec 2012; revised 18 Feb 2013; accepted 23 Feb 2013; published 4 Mar 2013

simultaneous absorption of three photons. In the 3PL shown in Fig. 2(a), all the emission bands can be attributed to the electronic transitions between the energy levels of Tb^{3+} and emissions originating from the electronic transitions between the energy levels of Gd^{3+} are not observed. This phenomenon suggests the transfer of electrons generated via 3PA from Gd^{3+} to Tb^{3+} when these two ions are located close together. This mechanism has been proposed earlier to interpret the luminescence from the glass generated by single photon excitation [16–18]. From Fig. 4, it can be seen that part of the pump energy may be lost due to the electronic absorption in the glass, reducing the efficiency of 3PL. In fact, the absorption at a short wavelength of ~267 nm cannot be avoided even for undoped glass. A possible way to reduce such absorption is to shift the pump light to a longer wavelength of ~820 nm (or ~936 nm). By doing so, we can resonantly induce the electric transition $^8S_{7/2} \rightarrow {}^6I_J$ (or $^8S_{7/2} \rightarrow {}^6P_{7/2}$) in Gd^{3+}, which corresponds to a wavelength of ~273 nm (or ~312 nm), through 3PA.

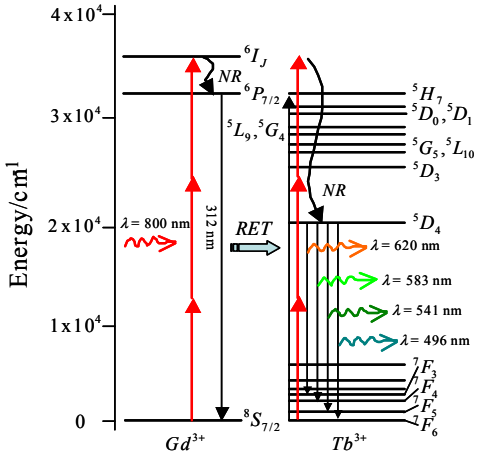

Fig. 3. Energy level diagrams for Gd^{3+} and Tb^{3+} showing the 3PA in Gd^{3+} and Tb^{3+} followed by nonradiative relaxation (NR), resonant energy transfer (RET) from Gd^{3+} to Tb^{3+}, and the electronic transitions between the energy levels of Tb^{3+} corresponding to the four emission bands observed in the MPL spectrum.

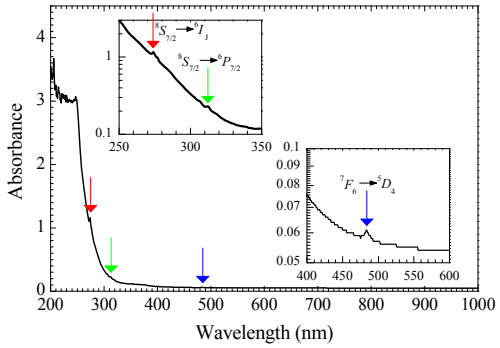

Fig. 4. Absorption spectrum of the glass in the ultraviolet, visible and near infrared regions. The red and green arrows indicate the absorptions in Gd^{3+} due to the electronic transitions $^8S_{7/2} \rightarrow {}^6I_J$ and $^8S_{7/2} \rightarrow {}^6P_{7/2}$ while the blue one indicates the absorption in Tb^{3+} due to the electronic transition $^7F_6 \rightarrow {}^5D_4$. The insets show the magnified spectral regions where the small absorption peaks can be identified. The vertical coordinate for each inset has been changed from linear to logarithmic in order to show clearly the absorption peaks.

#181857 - $15.00 USD Received 21 Dec 2012; revised 18 Feb 2013; accepted 23 Feb 2013; published 4 Mar 2013

3.3 Polarization dependence of the three-photon-induced luminescence

Keeping the physical mechanism for the 3PL in mind, let us examine the polarization dependence of the 3PL. In experiments, we changed the polarization of the fs laser by rotating the λ/2 plate placed outside the microscope. The reason why we did the experiments by using an inverted microscope is that the system shown in Fig. 1 provides high excitation density (small focused laser spot) as well as efficient collection of the generated luminescence. Similarly experiment was also carried out without using the microscope and polarization dependent luminescence was also demonstrated. However, the polarization dependence is not as strong as that observed by using the microscope because of the low excitation density and collection efficiency.

Initially, the laser light is horizontally polarized (θ = 0°) and it corresponds to a *s*-polarized wave for the dichroic mirror. If we make it vertically polarized (θ = 90°) by rotating the λ/2 plate by 45°, then it corresponds to a *p*-polarized wave. For both *s*- and *p*-polarized waves, their linear polarization states are preserved after being reflected by the dichroic mirror and focused by the objective lens. Accordingly, linearly polarized light along 0° (E_y') or 90° (E_x') can be obtained on the focused plane (see Fig. 1). In order to see the effects of polarization on the 3PL of the glass, we chose to generate an elliptically polarized light by utilizing the reflection phase difference between the *s*- and *p*-polarized waves. It was achieved by changing the polarization of the incident light before the dichroic mirror. The polarization states on the focused plane measured for different polarization angles (θ = 0°, 30°, 45°, 60°, and 90°) by using the combination of a Glan-Taylor polarizer and a power meter are shown in Fig. 5(a). Two linearly polarized beams along 0° and 90° and three elliptically polarized beams with different ellipticities are clearly identified.

In order to find out the effects of polarization on the 3PL intensity of the glass, we have recorded the 3PL spectra under different polarization states by simply rotating the λ/2 plate. The polarization dependent 3PL intensities at the central wavelengths of the four emission bands are presented in Fig. 5(b). For all emission bands, a periodic variation of the 3PL intensity with the change of the polarization angle is observed and the period is found to be 90°. Minima in the 3PL intensity are found to appear at *N* x 45°, where *N* is an integer. The 3PL intensity at minima is only one-fourth of that at maxima occurring at *N* x 90°. In this case, the excitation light is elliptically polarized as shown in Fig. 5(a). It implies that the up-conversion efficiency for elliptical polarization is lower than that for linear polarization. Since the 3PL originates from the 3PA in Gd^{3+} and Tb^{3+}, it is thought that the 3PA processes in Gd^{3+} and Tb^{3+} depend on the polarization of the excitation light. Actually, polarization dependent two-photon luminescence (2PL) has been observed in Gd^{3+}- and Eu^{2+}-doped crystals [19–22]. While the 2PA of most electronic transitions can be well interpreted by the second-order perturbation theory, a large discrepancy was found between the theoretical analysis and the experimental observation for some electronic transitions [19]. To the best of our knowledge, this puzzle has not been solved yet. Different from the previous experiments which were carried out in rare-earth-ion-doped crystals, we studied a rare-earth-doped glass in which the effects of site symmetry and crystal field are absent because glass is optically isotropic. By excluding such effects, the polarization dependent 3PA can only be interpreted by the anisotropy of the electronic transitions involved in the 3PA processes of Gd^{3+} and Tb^{3+} and/or by the angular distribution of photogenerated electrons in the glass which has been observed previously in Ge-doped silica glass [23]. However, more experiments are needed to clarify this important issue. Another difference we want to emphasize here is the excitation polarization dependent 3PL is observed in all emission bands. In rare-earth-ion-doped crystals, however, this kind of polarization dependence was observed only for some specific electronic transitions [19]. This feature provides another evidence for the RET from Gd^{3+} to Tb^{3+} because the polarization dependent 3PL is determined mainly by the polarization dependent 3PA in Gd^{3+} because of the large amount of Gd^{3+} doped in the glass.

#181857 - $15.00 USD Received 21 Dec 2012; revised 18 Feb 2013; accepted 23 Feb 2013; published 4 Mar 2013

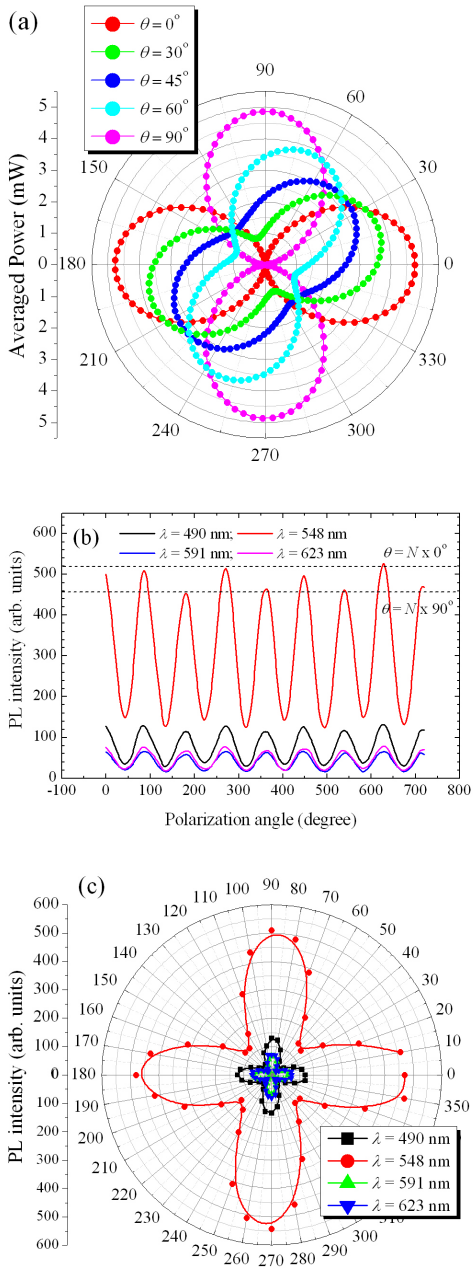

Fig. 5. (a) Polarization states of the fs laser light with polarization angles of 0°, 30°, 45°, 60°, and 90° after being reflected by the dichroic mirror. (b) Polarization dependent 3PL intensities at the central wavelengths of the four emission bands. (c) Excitation polarization dependent 3PL intensities at the central wavelengths of the four emission bands plotted in a polar coordinate.

In order to clearly show the polarization dependent 3PL from the glass, we have plotted the 3PL intensity as a function of polarization in a polar coordinate, as shown in Fig. 5(c). Another feature that is worth noting in Fig. 5(b) is the small difference in the 3PL intensity for the two linear polarizations perpendicular to each other. It is found that the 3PL intensity for

#181857 - $15.00 USD Received 21 Dec 2012; revised 18 Feb 2013; accepted 23 Feb 2013; published 4 Mar 2013

the polarization at 0° is about 1.1 times of that at 90°. This feature is not obvious for the emission bands with weak intensities (λ = 490, 591, and 623 nm) but it becomes significant for the emission band with the strongest intensity (λ = 549 nm). Actually, the reflectance of the dichromic mirror for *s*- and *p*-polarized waves is generally different. In our case, this difference is quite small and it cannot be resolved when we compared the power of the *s*- and *p*-polarized waves after the dichromic mirror (see Fig. 5(a)). However, the third power dependence of the 3PL on excitation density makes it possible for discriminating the small difference because it is quite sensitive to the small change in the excitation intensity. In addition, the efficient 3PL further enlarges the difference which can be easily identified in Fig. 5(b). Based on the difference in 3PL intensity, it is deduced that the power of *p*-polarized wave is about 1.03 times that of *s*-polarized one after being reflected by the dichroic mirror.

4. Summary

In summary, we have investigated the MPL from a scintillating silicate glass co-doped with Gd^{3+} and Tb^{3+} by using a focused fs laser light at 800 nm. The efficient upconversion luminescence appearing in the visible region was demonstrated to be 3PL and the physical mechanism is thought to be the 3PA in Gd^{3+} and Tb^{3+} followed by RET from Gd^{3+} to Tb^{3+}. A strong polarization dependence of 3PL was observed and it is attributed to the polarization dependent 3PA in Gd^{3+} and Tb^{3+} and/or the angular distribution of photogenerated electrons in the glass. The efficient MPL from rare-earth-ion-doped glass is expected to find applications in various fields of science and technology.

Acknowledgments

The authors acknowledge the financial support from the National Natural Science Foundation of China (Grant Nos. 10974060, 51171066 and 11111120068), the Ministry of Education (Grant No. 20114407110002) and the program for high-level professionals in the universities of Guangdong province, China.

#181857 - $15.00 USD Received 21 Dec 2012; revised 18 Feb 2013; accepted 23 Feb 2013; published 4 Mar 2013